Development 129, 5647-5658

doi:10.1242/dev.00162

Domain-specific olivocerebellar projection regulated by the EphA-ephrin-A interaction

Kazuhiko Nishida[1], John G. Flanagan[2] and Masaru Nakamoto[1,*]

[1]Department of Neurosciences, Lerner Research Institute, The Cleveland Clinic Foundation, Cleveland, OH 44195, USA
[2]Department of Cell Biology and Program in Neuroscience, Harvard Medical School, Boston, MA 02115, USA
*Author for correspondence (e-mail: nakamom@ccf.org)

Accepted 11 September 2002

SUMMARY

Neural maps in the vertebrate central nervous system often show discontinuously segregated, domain-to-domain patterns. However, the molecular mechanism that establishes such maps is not well understood. Here we show that in the chicken olivocerebellar system, EphA receptors and ephrin-As are expressed with distinct levels and combinations in mapping domains. When ephrin-A2 is retrovirally overexpressed in the cerebellum, the olivocerebellar map is disrupted, excluding axons with high receptor activity from ectopic expression domains. Conversely, overexpression of a truncated EphA3 receptor in the cerebellum reduces endogenous ligand activity to undetectable levels and causes aberrant mapping, with high receptor axons invading high ligand domains. In vitro, ephrin-A2 inhibits outgrowth of inferior olive axons in a region-specific manner. These results suggest that Eph receptors and ephrins constitute domain-specific positional information, and the spatially accurate receptor-ligand interaction is essential to guide inferior olive axons to their correct target domains.

Key words: Eph receptors, Ephrins, Olivocerebellar projection, CNS

INTRODUCTION

The correct functioning of the nervous system is critically dependent upon the establishment of precise connections between neurons and their target cells. In the vertebrate nervous system, axon projections are usually arranged in an orderly manner in which location of neurons in the projecting field is reflected in their connections in the target field. The mode of arranging projecting axons to the target cells varies depending on neuronal pathways, from a graded, continuous mapping to a more complex, discontinuously segregated pattern. The retinotectal projection is an extreme example of the former type, in which the temporal-to-nasal and dorsal-to-ventral axes of the retina map smoothly along the anterior-to-posterior and ventral-to-dorsal axes of the tectum, respectively. This type of topographic mapping provides a way for the nervous system to transfer information from one area to another, while faithfully preserving its original spatial order, and may therefore be more suitable to first-order sensory systems, where the format of information transfer can be relatively simple. Since first proposed by Sperry in the chemoaffinity theory (Sperry, 1963), it has been shown by experimental and theoretical research that the initial development of this continuously graded map can be established by gradients of complementary identification tags that bear positional information in the projecting and target fields (Thanos and Mey, 2001)

In contrast, neural areas that are involved in higher-order information processing, such as multisensory integration and sensorimotor integration, require more complex projection patterns. One of the common ways used to build up the central neural maps is to arrange the incoming afferent fibers into distinct domains in the target region, as seen in the mosaic of two compartments (the patches and matrix) in the striatum, and in the modular columnar organization in the cerebral cortex. However, little is known about the molecular mechanisms that establish such discontinuous maps. Interestingly, although it has long been thought that neuronal activity plays the main role in development of the cortical columnar organization, recent studies have suggested that the formation of ocular dominance column in the visual cortex may also be dependent on molecular cues (Crowley and Katz, 2000).

The neuronal projection from the inferior olive (IO) in the myelencephalon to the cerebellum has been used as a favorite model system to study domain-specific neural maps (the olivocerebellar projection) (Altman and Bayer, 1997; Brodal and Kawamura, 1980). Previous studies have revealed that the axons of IO neurons project to Purkinje cells in the contralateral side of the cerebellum, with at least two overlapping patterns. First, IO axons are organized along the rostrocaudal axis of the cerebellum (Furber, 1983; Furber and Watson, 1983). In chicken, neurons in the rostromedial IO project to the caudal cerebellum, while neurons in the caudolateral IO project to the rostral cerebellum (Chédotal et al., 1997; Furber, 1983). Second, discrete areas of the IO project to different domains in the cerebellar cortex that

are aligned mediolaterally (parasagittal domains) (Buisseret-Delmas and Angaut, 1993). Whereas this mediolateral arrangement is ordered with respect to the local origin of IO neurons, neighboring domains of the IO do not always project to adjacent cerebellar domains, thus forming a discontinuous mapping with sharp boundaries. Although it has been predicted that the matching of domain-specific labels between the incoming axons and target cells would be the mechanism for the formation of the olivocerebellar projection (Sotelo and Chédotal, 1997; Wassef et al., 1992), the molecular nature of such labels remains to be elucidated.

In recent years, Eph receptor tyrosine kinases and their membrane-bound ligands, ephrins, have been implicated in neuronal network formation. Both the Eph and ephrin families can be divided into two groups based on structural features and binding affinities; i.e. EphA1-A9, EphB1-B6, ephrin-A1-A6 (glycosyl phosphatidylinositol (GPI)-anchored), and ephrinB1-B3 (transmembrane) (Eph Nomenclature Committee, 1997; Menzel et al., 2001) [see Eph nomenclature web site (http://cbweb.med.harvard.edu/eph-nomenclature/) for update]. With a few exceptions, the groupings of the Eph receptors and ephrins correspond to the receptor-ligand interaction (ephrin-A ligands preferentially bind to EphA receptors, and ephrin-B ligands to EphB receptors), although there are wide variations in affinity within each group (Flanagan and Vanderhaeghen, 1998). Their functions in neuronal projection are most typically shown in development of the retinotectal (retinocollicular, in mammals) system. In this system, EphA receptors and ephrin-A ligands are expressed in complementary gradients along the anteroposterior axes of the projecting and target fields, respectively (Cheng et al., 1995; Drescher et al., 1995). The receptor-ligand interaction mediates topographically specific repulsive signals, and thus acts as a major determinant of this continuously graded neuronal projection (Feldheim et al., 2000; Monschau et al., 1997; Nakamoto et al., 1996). While many central neural maps show discontinuously segregated patterns, however, whether or how the Eph-ephrin system acts as the molecular mechanism to establish such domain-specific projections is still unknown. In the present study, we performed expression analyses and functional characterization of Eph receptors and ephrins in the chicken olivocerebellar system. Our results suggest that in the olivocerebellar projection, EphA receptors and ephrin-A ligands provide domain-specific positional information that guides axons to their correct target domains.

MATERIALS AND METHODS

RNA in situ hybridization and affinity probe in situ

For RNA probe preparation, cDNA fragments of *EphA5* (nucleotide 910-1725) (Siever and Verderame, 1994), *EphA6* (nucleotide 455-1170; DDBJ accession number, AB083185), and *ephrin-A5* (nucleotide 25-791) (Drescher et al., 1995) were amplified by RT-PCR from E10 chick brain total RNA, and were subcloned into pBluescript-SK(–) (Stratagene) or pCRII (Invitrogen). The probes for *EphA3* and *ephrin-A2* have been described previously (Cheng et al., 1995). In situ hybridization using digoxigenin-labeled RNA probes and affinity probe in situ was performed as described previously (Cheng et al., 1995). For histological analyses, 30 μm frozen sections of the hindbrain were used.

Organotypic hindbrain cultures

Organotypic cultures of the chicken hindbrain were performed basically as previously described (Chédotal et al., 1997), except that we prepared explants at E9 or 10, by which time the domain patterns in the cerebellum can be clearly identified.

Axon tracing experiments

A tiny crystal of DiI and DiA (Molecular Probes) was injected into different domains of either the IO or the cerebellum in the organotypic hindbrain culture on the first to forth day in vitro (corresponding to E9-12 in ovo). After incubation for 64-72 hours (anterograde tracing) or for 40-48 hours (retrograde tracing), projection patterns were analyzed under a fluorescence microscope. Using the same explants, affinity probe in situ (with EphA3-AP or ephrin-A2-AP) or RNA in situ hybridization was performed to determine exact insertion sites of axon tracers and labeled neurons. In retrograde labeling, 30 μm-frozen sections through the IO were cut, and subjected to RNA in situ hybridization with *EphA* probes.

Retrovirus preparation and injection

Retrovirus stocks of RCAS-ephrin-A2, RCAS-EphA3ΔC, and RCAS-AP were prepared as described previously (Fekete and Cepko, 1993a; Nakamoto et al., 1996). RCAS-EphA3ΔC contains chicken EphA3 sequences from nucleotide 173-1756 fused to short 5′coding region derived from mouse EphA3 cDNA (nucleotide 89-235) (Sajjadi et al., 1991) in a retroviral vector RCASBP(B) (Fekete and Cepko, 1993b). The virus solution with dye tracer was injected into the rostral hindbrain region of E2 [Hamburger and Hamilton stage (HH) 10-12] chick embryos in windowed eggs. Virus-mediated expression was evaluated by RNA in situ hybridization, affinity probe in situ, or alkaline phosphatase (AP) staining. Only the explants in which the virus-derived gene expression was restricted to the cerebellum were used for the axon tracing experiments.

In vitro membrane substratum assay

The membrane substratum assay was performed as previously described (Frisén et al., 1998). Briefly, 293T cell membranes were prepared 68-72 hours after transfection with pcDNAI-ephrin-A2 or pcDNAI control plasmid (Invitrogen) using the calcium phosphate method, and were mixed with membranes from the anterior third of E8 tecta (2:1) to create a more permissive growth substratum. Medial or lateral IO explants (175 μm in width, 500 μm in length) were prepared from E8 embryos, and were placed onto the homogeneous membrane carpets. After 60 hours, neurite outgrowth was scored on a graded 0-4 scale, in which 0 was no or very sparse outgrowth from a living explant and 4 was very robust growth. Statistical significance of the data was determined using Student's unpaired *t*-test.

RESULTS

Multiple EphA receptors are expressed in the IO with distinct and overlapping patterns

In chicken, IO axons enter the cerebellum at embryonic day 8.5-9 (E8.5-9), and initial target selection takes place around E10 (Chédotal et al., 1996). To explore the possibility that Eph receptors act as positional cues in the domain-specific olivocerebellar projection, we first examined their expression patterns in the IO at these developmental stages by RNA in situ hybridization. Significant mRNA expression of *EphA3, EphA5*, and *EphA6* was detected at E8, and high expression continued to be seen on E10, E12 and E14 (expression at E10 is shown in Fig. 1). *EphA3* was expressed in a narrow area in the medial part of the IO, extending along almost the entire rostrocaudal axis of the nucleus (Fig. 1A,D,H,L). In contrast, *EphA5*

showed a broader expression in the medial part of the IO (Fig. 1B,E,I,M). Within the expression domain, *EphA5* expression was particularly strong in the caudolateral and caudomedial parts (arrowheads in Fig. 1I). Expression of *EphA6* in the IO was restricted in the most medial part rostrally, but was seen in a broader area caudally (Fig. 1C,F,J,N).

Based on the expression patterns of *EphA3*, *EphA5* and *EphA6*, at least four classes of IO areas could be distinguished (Fig. 1P,Q): (i) EphA3-positive, EphA5-positive, EphA6-positive (EphA3(+), EphA5(+), EphA6(+)) area in the medial part of the IO (Area Ml); (ii) EphA3-negative, EphA5-strong positive, EphA6-positive (EphA3(–), EphA5(++), EphA6(+)) areas in the caudal part of the intermediate region (Area Ic) and in the most medial part of the IO (Area Mm); (iii) EphA3-negative, EphA5-positive, EphA6-negative (EphA3(–), EphA5(+), EphA6(–)) area in the rostral-intermediate region (Area Ir); and (iv) EphA3-negative, EphA5-negative, EphA6-negative (EphA3(–), EphA5(–), EphA6(–)) region in the lateral part of the IO (Area L).

Ligand-AP detects receptor activity that corresponds to the area-specific mRNA expression patterns

Since the interaction between Eph receptors and ephrins is promiscuous, with a single ligand binding multiple receptors with different affinities, we were next interested in evaluating how the expression of EphA receptors was reflected on the total receptor activity in each IO area. To test this, we performed affinity probe in situ (Cheng et al., 1995), in which the extracellular domain of ligands fused to an AP-tag was used as a probe to detect the distribution of receptor activity (Fig. 1G,K,O).

As expected, an ephrin-A2-AP probe detected a high receptor activity in Area Ml (EphA3(+), EphA5(+), EphA6(+)). Interestingly, Areas Ic and Mm (EphA3(–), EphA5(++), EphA6(+)) also showed strong receptor activity that was comparable to that in Area Ml, presumably reflecting the strong expression of *EphA5*. Weak receptor activity was observed in Area Ir (EphA3(–), EphA5(+), EphA6(–)), whereas no activity could be seen in Area L (EphA3(–), EphA5(–), EphA6(–)). No binding activity was detectable for ephrin-B2-AP (K. N. and M. N., unpublished), suggesting that EphB receptors are not expressed at significant levels in the IO. The results showed that ligand-AP could indeed detect receptor activity in the IO that correlated with the expression patterns revealed by RNA in situ hybridization.

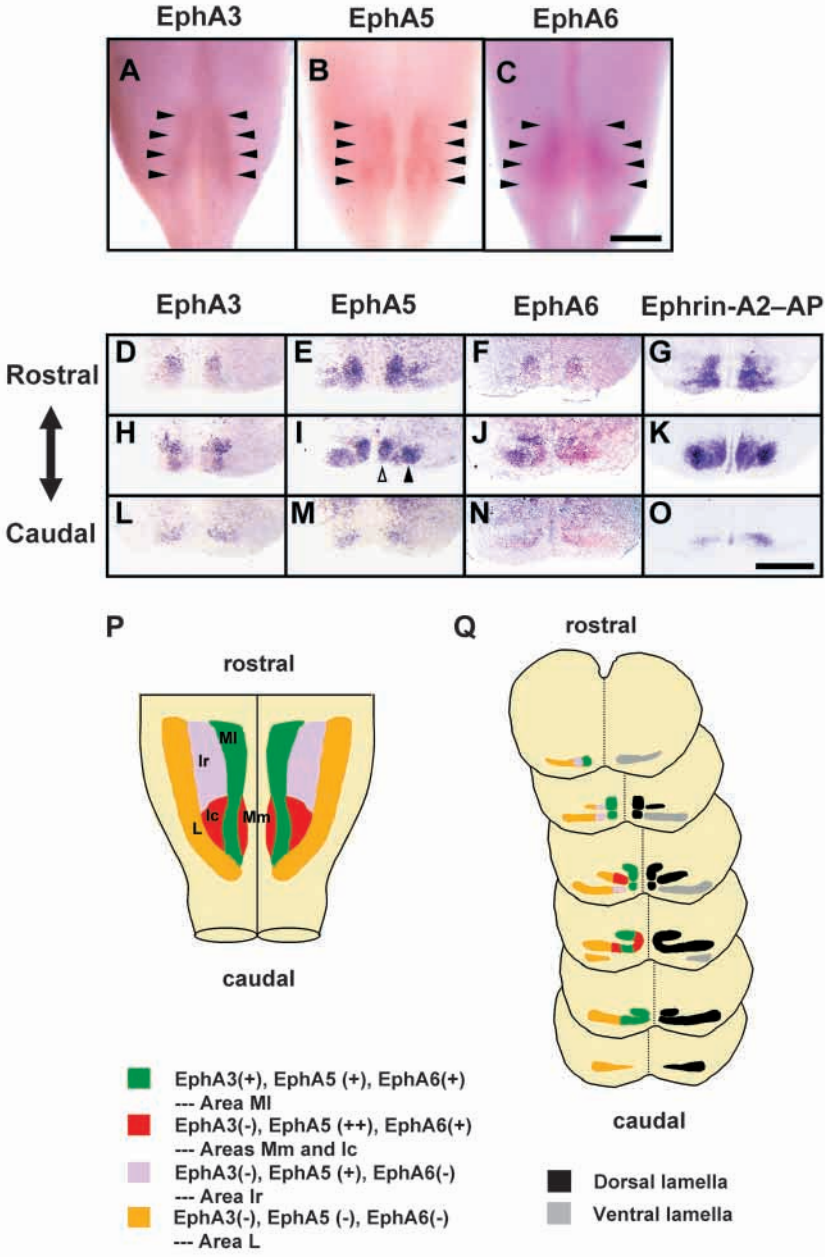

Fig. 1. Expression and activity of EphA receptors in the E10 chick IO. (A-C) Whole-mount RNA in situ hybridization of the brainstem. Ventral views are shown. Rostral is at the top. Arrowheads indicate expression in the IO. (D-O) Coronal sections through the IO subjected to RNA in situ hybridization (D-F, H-J, L-N) or affinity probe in situ (G,K,O). Dorsal is at the top. *EphA3* is expressed in a narrow area of the medial IO, whereas *EphA5* and *EphA6* show broader distribution. White and black arrowheads in I indicate areas Mm and Ir, respectively, which show strong *EphA5* expression. Total receptor activity detected with ephrin-A2-AP corresponds to the RNA expression patterns. Scale bars: 500 μm. (P-Q) Areas defined by EphA receptor expression are schematized in a ventral view of the brainstem (P) and serial coronal sections (Q, left side). Lamellar organization of the IO is shown on the right side of Q.

Domains of cerebellar Purkinje cells detected by expression and activity of ephrin-A ligands

It has recently been shown immunohistochemically that the ephrin-A2 and ephrin-A5 proteins are distributed in parasagittal domains of Purkinje cells in the developing chicken cerebellum (Karam et al., 2000). In the present study, to directly relate their expression patterns to the olivocerebellar

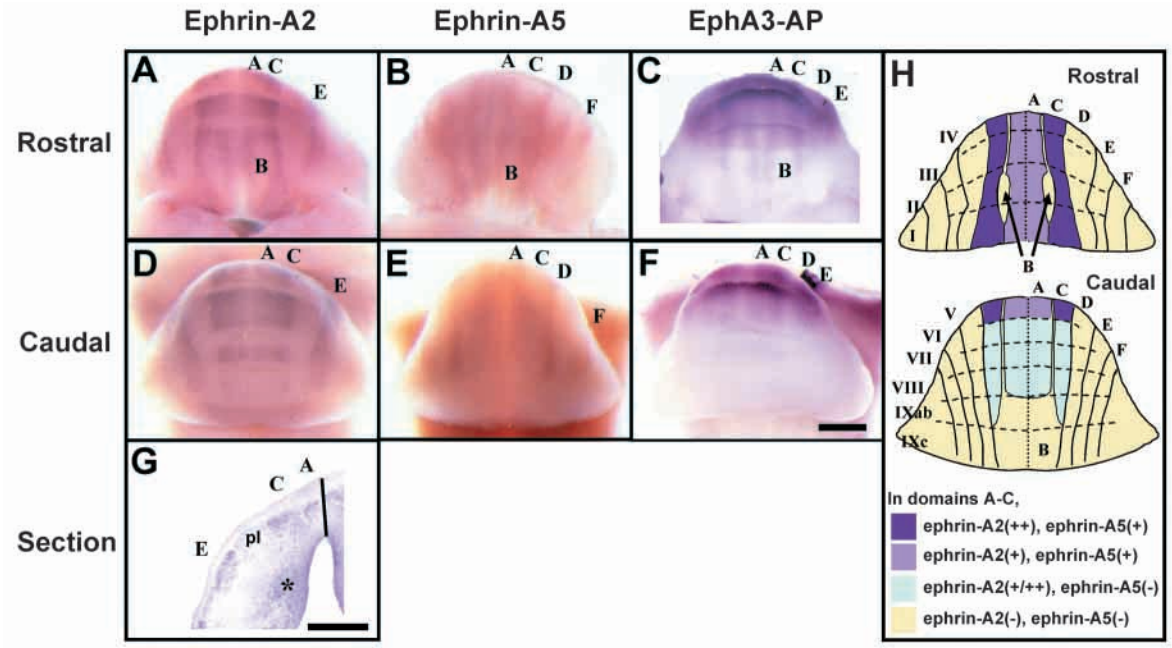

Fig. 2. Expression and activity of ephrin-A ligands in the E10 cerebellum. (A-F) RNA in situ hybridization (A,B,D,E) and affinity probe in situ (C,F) of whole mount cerebellum. Capital letters indicate domain names. (A-C) Dorsal is at the top. (D-F) Anterior is at the top. Expression of *ephrin-A2* is strongest in domain C (lobules I-IXab), followed by domain A (lobules I-VIII) and E (lobules II-VII). *ephrin-A5* is moderately expressed in domains A (lobules I-V), C (lobules I-V), D (lobules I-VIII) and F (lobules III-VIII). Total ligand activity detected with an EphA3-AP probe corresponds to the RNA expression patterns. (G) *ephrin-A2* expression in a coronal section of the cerebellum (lobulus VII). Parasagittal pattern is seen in the Purkinje cell layer (pl). Asterisk, deep cerebellar nuclei. (H) A diagram of parasagittal domains in the cerebellum. Please note that expression patterns of *ephrin-A2* and *ephrin-A5* are shown only in domains A-C. Scale bars: 500 μm.

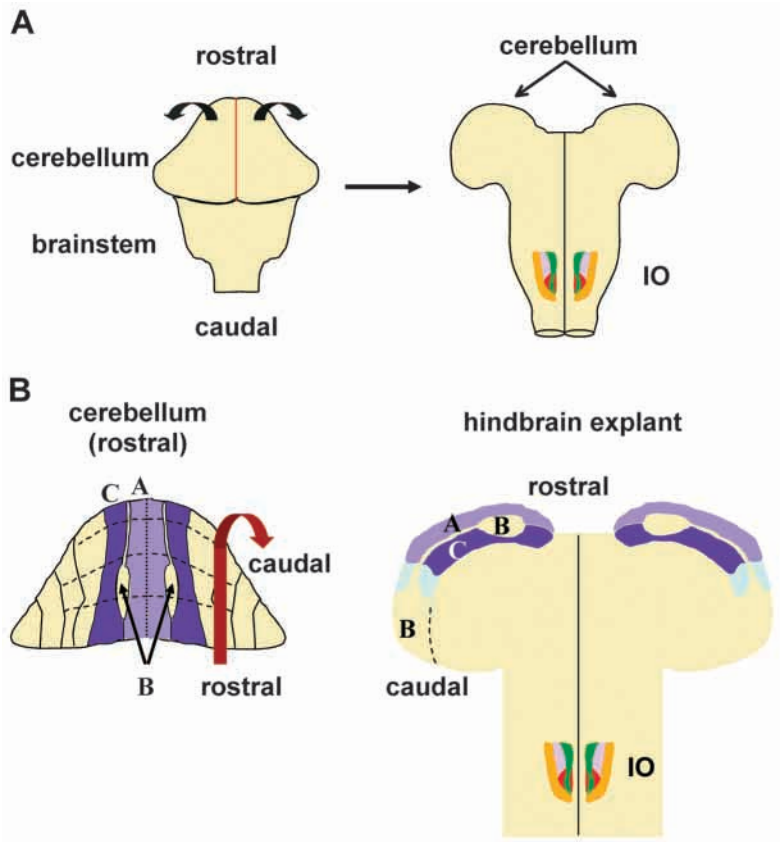

map, we re-examined expression of *ephrin-A2* and *ephrin-A5* in the chicken cerebellum by RNA in situ hybridization.

Based on the expression patterns, we named the parasagittal domains alphabetically from the midline to the lateral sides (domains A to F; Fig. 2H). At E10, *ephrin-A2* was most strongly expressed in domain C (lobules I-IXab), and moderately in domains A (lobules I-VIII) and E (lobules II-VII) (Fig. 2A,D). *ephrin-A5* was expressed in the rostral part of domains A and C (lobules I-V), and in domains D (lobules I-VIII) and F (lobules III-VIII) (Fig. 2B,E). No *ephrin-A2* or *ephrin-A5* expression was detected in domain B, which consists of the rostral oval region and the caudal polygonal region that are connected by a very narrow band. Consistent with the previous report (Karam et al., 2000), the parasagittal domains of *ephrin-A2* and *ephrin-A5* represent their

Fig. 3. Organotypic hindbrain culture. (A) The whole hindbrain containing the cerebellum and brainstem was isolated from E10 embryo. The cerebellum was cut along the dorsal midline (red line), and the both halves of the cerebellum were separated and turned over.
(B) Comparison of *ephrin-A* expression in domains A-C between the native cerebellum and explant. Dark purple: ephrin-A2(++), ephrin-A5(+) (rostral domain C). Light purple: ephrin-A2 (+), ephrin-A5(+) (rostral domain A). Light blue: ephrin-A2 (+ or ++), ephrin-A5(–) (middle parts of domains A and C).

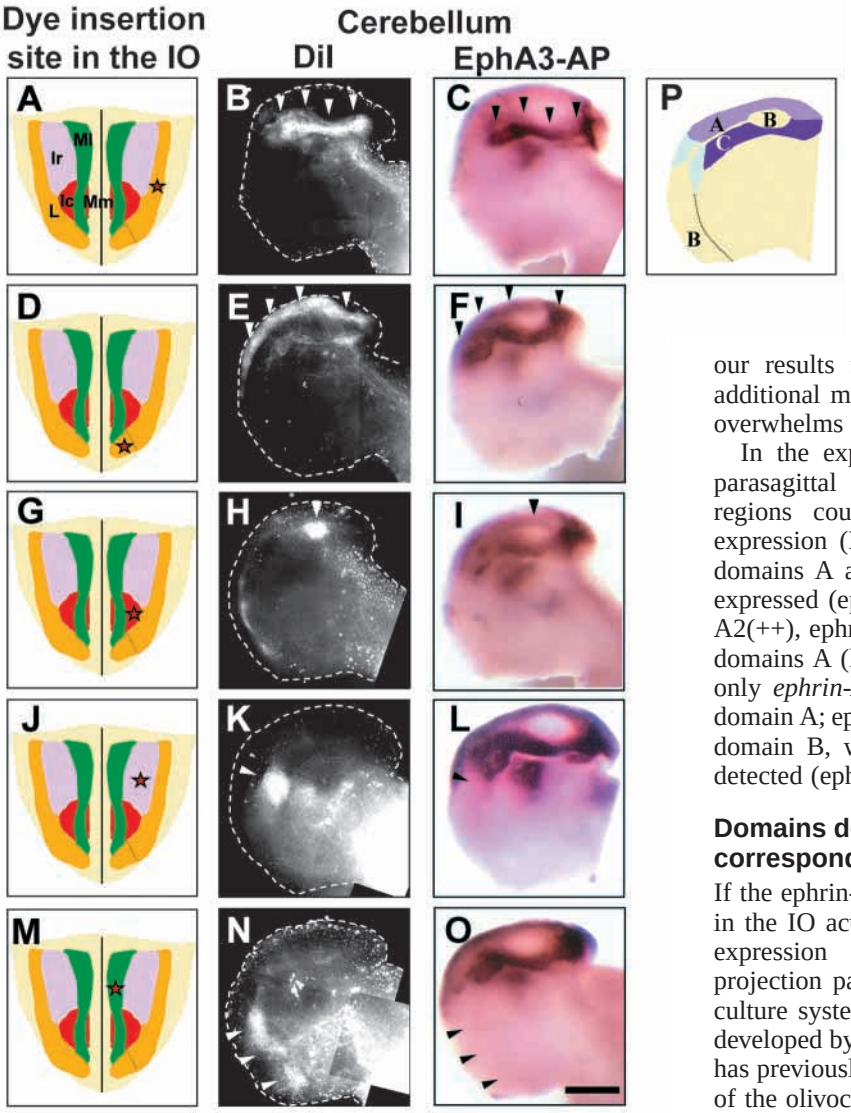

Fig. 4. Anterograde tracing of IO axons. (A,D,G,J,M) DiI insertion sites in the IO (red stars). Ventral views. IO areas are shown as in Fig. 1P. (B,E,H,K,N) Projection patterns of DiI-labeled axons (white arrowheads) in the contralateral side of the cerebellum. (C,F,I,L,O) Domain patterns of ligand activity detected with EphA3-AP. Black arrowheads indicate projection areas of DiI-labeled axons shown by white arrowheads in B,E,H,K,N. (P) Scheme of cerebellar domains in explant (see Fig. 3B). In each panel, rostral is at the top. (A-C) Axons from the main part of Area L project to the rostral parts of domain C. (D-F) The most caudal part of Area L maps to the rostral domain A. (G-I) Area Ic maps to the rostral oval region of domain B. (J-L) Area Ir maps to the middle region of domain C. (M-O) Area Ml maps to the caudal domain B. Scale bar, 500 μm.

expression in the Purkinje cell layer (Fig. 2G and data not shown).

Next, we tested how the ephrin-A ligand activity in the cerebellum is recognized by cognate EphA receptors by affinity probe in situ (Fig. 2C,F). Consistent with the RNA expression patterns, the rostral part of domain C (ephrin-A2(++), ephrin-A5(+)) showed strong ligand activity, followed by the rostral domains A (ephrin-A2(+), ephrin-A5(+)) and E (ephrin-A2(+), ephrin-A5(–)). Significant ligand activity was also observed in the rostral domain D (ephrin-A2(–), ephrin-A5(+)). Weak ligand activity was detected in the middle regions of domains A (ephrin-A2(+), ephrin-A5(–)) and C (ephrin-A2(++), ephrin-A5(–)) after longer incubation. No ligand activity was detected in domain B (ephrin-A2(–), ephrin-A5(–)).

It should be noted that since not all members of the Eph and ephrin families have been cloned in chicken, it is possible that other members are expressed in the IO or the cerebellum with distinct patterns. However, our results from affinity probe in situ indicate that such additional molecules, if any, are not expressed in a way that overwhelms the domain-pattern described above.

In the experiments described below, we focused on the parasagittal domains A-C in the cerebellum, where three regions could be distinguished based on the *ephrin-A* expression (Fig. 2H); (i) the rostral region (lobules I-V) of domains A and C, where both *ephrin-A2* and *ephrin-A5* are expressed (ephrin-A2(+), ephrin-A5(+) in domain A; ephrin-A2(++), ephrin-A5(+) in domain C); (ii) the middle region of domains A (lobules VI-VIII) and C (lobules VI-IXab), where only *ephrin-A2* is expressed (ephrin-A2(+), ephrin-A5(–) in domain A; ephrin-A2(++), ephrin-A5(–) in domain C); and (iii) domain B, where no *ephrin-A2* or *ephrin-A5* expression is detected (ephrin-A2(–), ephrin-A5(–)).

Domains defined by Eph receptors and ephrins correspond to olivocerebellar mapping domains

If the ephrin-A ligands in the cerebellum and EphA receptors in the IO act as domain-specific labels, it is likely that their expression patterns correlate with the olivocerebellar projection pattern. To study this, we utilized an organotypic culture system of the whole hindbrain, which was originally developed by Sotelo's group (Chédotal et al., 1996) (Fig. 3). It has previously been shown that in this system, the topography of the olivocerebellar projection is preserved (Chédotal et al., 1997). We have also confirmed that the domain patterns of EphA receptors and ephrins are preserved in the explants (data not shown and Figs 4-6).

In the organotypic hindbrain culture, we first performed anterograde tracing experiments by inserting a tiny crystal of DiI into different areas of the IO. When Area L (EphA3(–), EphA5(–), EphA6(–)) was marked with DiI, two different patterns were observed depending on the exact dye-insertion sites. In most cases, dense axonal plexures were detected in the rostral part of domain C (ephrin-A2(++), ephrin-A5(+)) (Fig. 4A-C). In contrast, if the most caudal part of Area L was marked, labeled axons projected to the rostral part of domain A (ephrin-A2(+), ephrin-A5(+)) (Fig. 4D-F). Axons from Area Ml (EphA3(+), EphA5(+), EphA6(+)) projected to the caudal part of domain B (ephirn-A2(–), ephrin-A5(–)) (Fig. 4M-O). Interestingly, when Area Ic (EphA3(–), EphA5(++), EphA6(+)) was marked, labeled axons were found to project to the rostral oval region of domain B (ephrin-A2(–), ephrin-A5(–)) (Fig. 4G-I). Finally, axons from Area Ir (EphA3(–), EphA5(+), EphA6(–)) were found to project to the middle region of domain C (ephrin-A2(++), ephrin-A5(–)) (Fig. 4J-L). No clear projection pattern was reproducibly obtained by marking Area Mm.

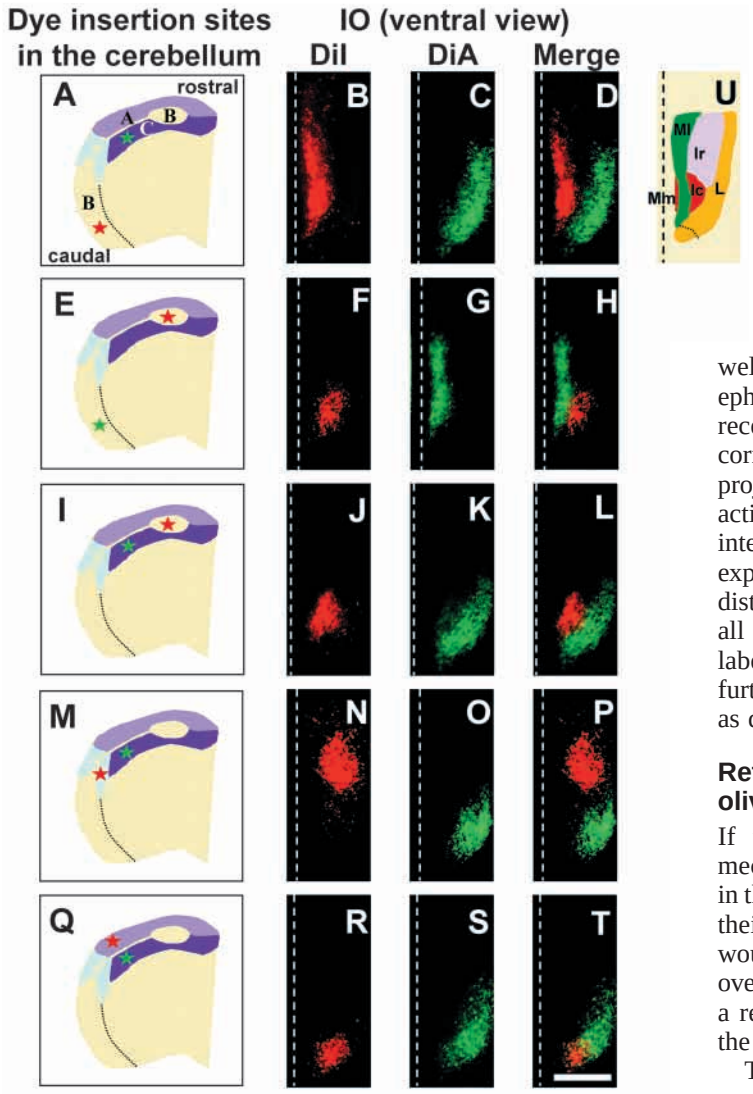

Fig. 5. Domain patterns of retrogradely labeled IO axons. (A,E,I,M,Q) A diagram of DiI (red star) and DiA (green star) insertion sites in one half of the cerebellum. (B-D,F-H,J-L,N-P,R-T) Retrogradely labeled neurons in the IO. Ventral views are shown. Rostral is at the top. Dashed line indicates the ventral midline. Scale bar, 500 μm. (U) A diagram of IO areas (see Fig. 1P).

To confirm the results of the anterograde labeling, we next performed retrograde axon tracing. In each explant, we inserted a crystal of two different dyes (DiI and DiA) into different cerebellar domains, so that the positional relationship between the labeled IO neurons would be clear.

The results were consistent with the anterograde labeling. When a dye crystal was inserted into the caudal part of domain B, labeled cells were detected in the medial part of the IO as a narrow band that extended rostrocaudally (Fig. 5B,D). To determine the identity of the labeled area, we cut sections through the IO of the labeled explant and performed RNA in situ hybridization with *EphA* probes. Both *EphA3* and *EphA5* RNAs were detected in the area, indicating that labeled cells were in Area Ml (Fig. 6A-D). In contrast, when the rostral part of domain C was marked, the labeled cells localized in the caudolateral part of the IO (Fig. 5C,D,K,L,O,P,S,T). In section RNA in situ hybridization, this part was identified to be in Area L, as neither *EphA3* nor *EphA5* was expressed there (Fig. 6M-P). The most caudal part of Area L was labeled when the dye was inserted into the rostral domain A (Fig. 5R,T, Fig. 6Q-T). Similarly, the middle region of domain C received axons from Area Ir (Fig. 5N,P, Fig. 6I-L). Finally, when the rostral oval region of domain B was marked, labeled cells were identified in Area Ic of the IO (Fig. 5F,H,J,L, Fig. 6E-H).

Taken together, the axon tracing experiments revealed that in the olivocerebellar projection, the projecting areas in the IO defined by EphA receptor expression correlate well with the target domains in the cerebellum defined by ephrin-A ligand expression (summarized in Fig. 7). First, the receptor and ligand expressions were in a reciprocal or inverse correlation; areas in the IO with high EphA receptor activity project to cerebellar domains with no or low ephrin-A ligand activity, and vice versa, suggesting that the receptor-ligand interaction mediates repulsive signals. Second, IO areas expressing different combinations of Eph receptors mapped to distinct cerebellar domains. It is also important to note that in all different retrograde labeling combinations, DiI- and DiA-labeled areas in the IO do not overlap, but are complementary, further supporting the idea that Eph receptors and ephrins act as domain-specific molecular labels.

Retroviral misexpression of ephrin-A2 disrupts the olivocerebellar projection pattern

If the Eph-ephrin interaction functions as the molecular mechanism that guides IO axons to their correct target domains in the cerebellar cortex, it would be expected that by modifying their expression patterns, the olivocerebellar projection pattern would be altered correspondingly. To test this possibility, we overexpressed *ephrin-A2* in the developing cerebellum, using a retrovirus-mediated gene expression system, and examined the effects on the projection pattern.

The RCAS-ephrin-A2 retrovirus (Nakamoto et al., 1996) was injected into the hindbrain region of the neural tube at E2 in ovo (HH 10-12). We took care to localize the virus infection to the rostral part of the hindbrain, from which the cerebellum develops. Efficiency and patterns of ectopic expression were examined later by affinity probe in situ using an EphA3-AP probe. As shown in Fig. 8B, the vast majority of cerebella infected with the virus showed massive *ephrin-A2* expression that covered most of the cerebellar surface.

We next tested for effects of ectopic *ephrin-A2* expression on the projection pattern, by retrograde labeling in explants prepared from virus-infected embryos. In each explant, we double-labeled the rostral domain C (ephrin-A2(++), ephrin-A5(+)) and the caudal domain B (ephrin-A2(–), ephrin-A5(–)). After infection with a negative control virus RCAS-AP (n=28), the labeling patterns in the IO were indistinguishable from those observed in wild type (uninfected) explants (Fig. 8G-I). In contrast, 85% (22/26) of the explants infected with the RCAS-ephrin-A2 virus showed aberrant projection patterns. In most of the aberrant cases (18/26), the caudal part of domain B was invaded by axons from more lateral parts of the IO, and only a small number of Area Ml neurons projected there (Fig. 8J-L). Only in some cases (4/26), significant numbers of Area Ml cells were labeled together with cells in the lateral parts (data not shown). These results indicate that when *ephrin-A2*

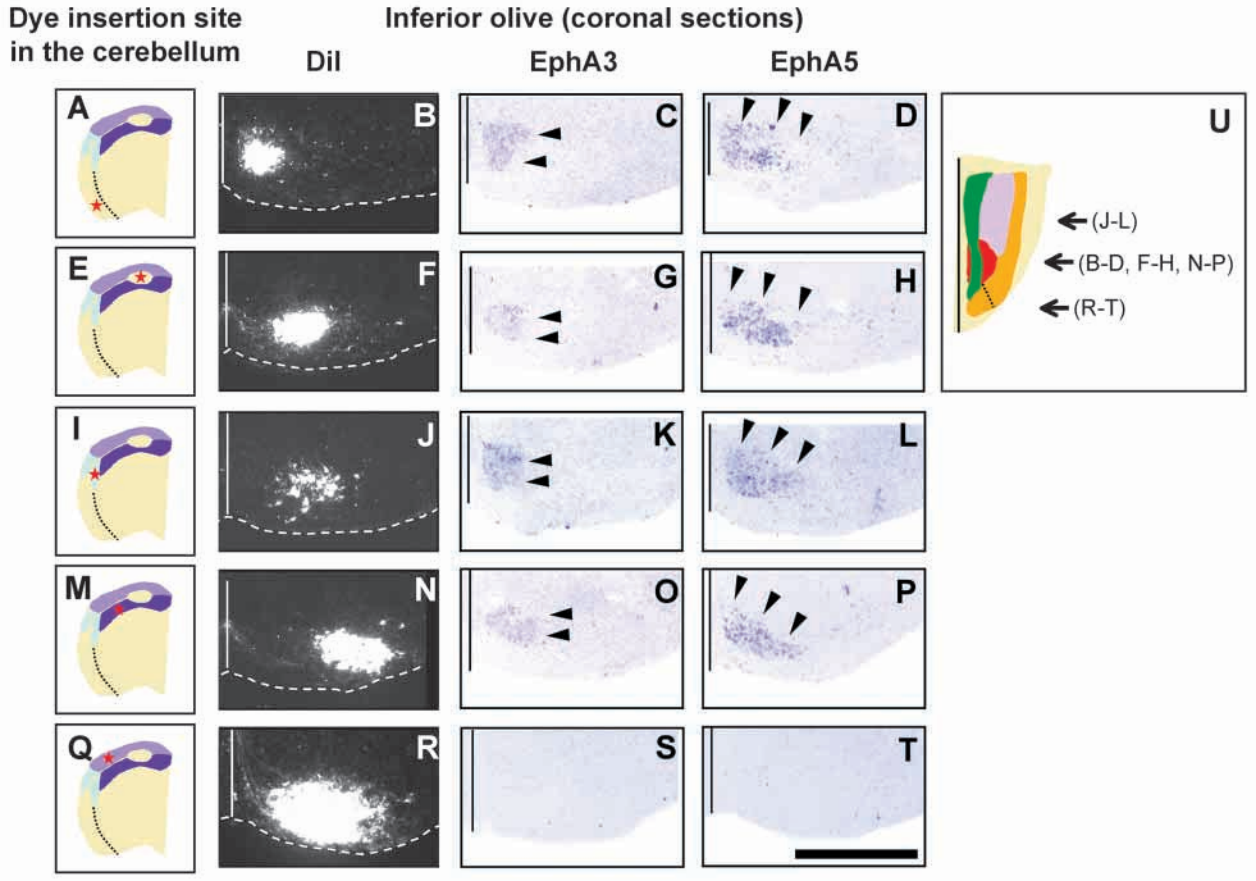

Fig. 6. EphA receptor expression profiles of retrogradely-labeled areas in IO. (A,E,I,M,Q) DiI insertion sites (red star) in the cerebellum. (B,F,J,N,R) Retrogradely labeled neurons in the contralateral IO. Dashed lines indicate ventral outlines of the brainstem. Dorsal is at the top. Vertical lines indicate midline. (C,D,G,H,K,L,O,P,S,T) *EphA3* and *EphA5* expression detected by RNA in situ hybridization in the same and adjacent coronal sections through the IO (arrowheads). Scale bar, 500 μm. (U) A diagram indicating the positions of coronal planes of the sections. (A-D) The caudal domain B is innervated by axons from the medial IO, where both *EphA3* and *EphA5* are expressed (Area Ml). (E-H) The rostral domain B receives axons from the caudo-intermediate IO, where no *EphA3*, but strong *EphA5* expression is detected (Area Ic). *EphA6* is also expressed in this area (data not shown). (I-L) The middle region of domain C receives axons from the rostro-intermediate IO, where no *EphA3* and moderate *EphA5* expression is detected (Area Ir). *EphA6* expression was not detected in this area (data not shown). (M-T) The rostral parts of domains C and A receive axons from the lateral IO, where both *EphA3* and *EphA5* are not expressed (Area L).

is overexpressed in the developing cerebellum, most Area Ml axons fail to project to the normal target domain (the caudal domain B), and lateral IO axons project to not only their normal target domain, but also the caudal domain B. Consistent with these results, when axons of Area Ml were anterogradely-labeled, the labeled axons stalled on the ventral border of the cerebellum (Fig. 8Q,R), suggesting that ectopic *ephrin-A2* expression prevents Area Ml axons from entering the cerebellum.

Ephrin-A2 inhibits outgrowth of IO axons in vitro in a region-specific manner

Our in vivo results suggest that ephrin-A2 prevents IO axons with high receptor activity from invading cerebellar domains with high ligand activity, through repulsion or growth inhibition of axons. To directly test this, we used an in vitro membrane substratum assay (Frisén et al., 1998; Walter et al., 1987). Since it is not readily feasible to separate individual areas of the IO with reasonable reproducibility, we instead compared axonal behavior between the medial (high EphA receptor activity) and lateral (low to no EphA receptor activity) parts of the IO. The medial and lateral parts of the IO were separately dissected out, and were cultured on homogeneous membrane carpets prepared from ephrin-A2- or mock-transfected 293T cells (Fig. 9).

Axon outgrowth from lateral IO explants showed no significant difference between on control [n=17, score 3.6±0.1(s.e.m.)] and ephrin-A2 [n=18, score 3.6±0.1(s.e.m.)] membranes. In contrast, axon outgrowth from the medial IO was significantly inhibited on the ephrin-A2 membrane [n=17, score 1.3±0.3(s.e.m.)], compared to the control membrane [n=13, score 2.6±0.3, P<0.001) These results indicate that ephrin-A2 inhibits growth of IO axons in a region-specific manner.

Retroviral overexpression of a truncated EphA3 receptor significantly reduces the ephrin-A ligand activity in the cerebellum and causes aberrant olivocerebellar projection

In the developing chicken cerebellar cortex, several EphA

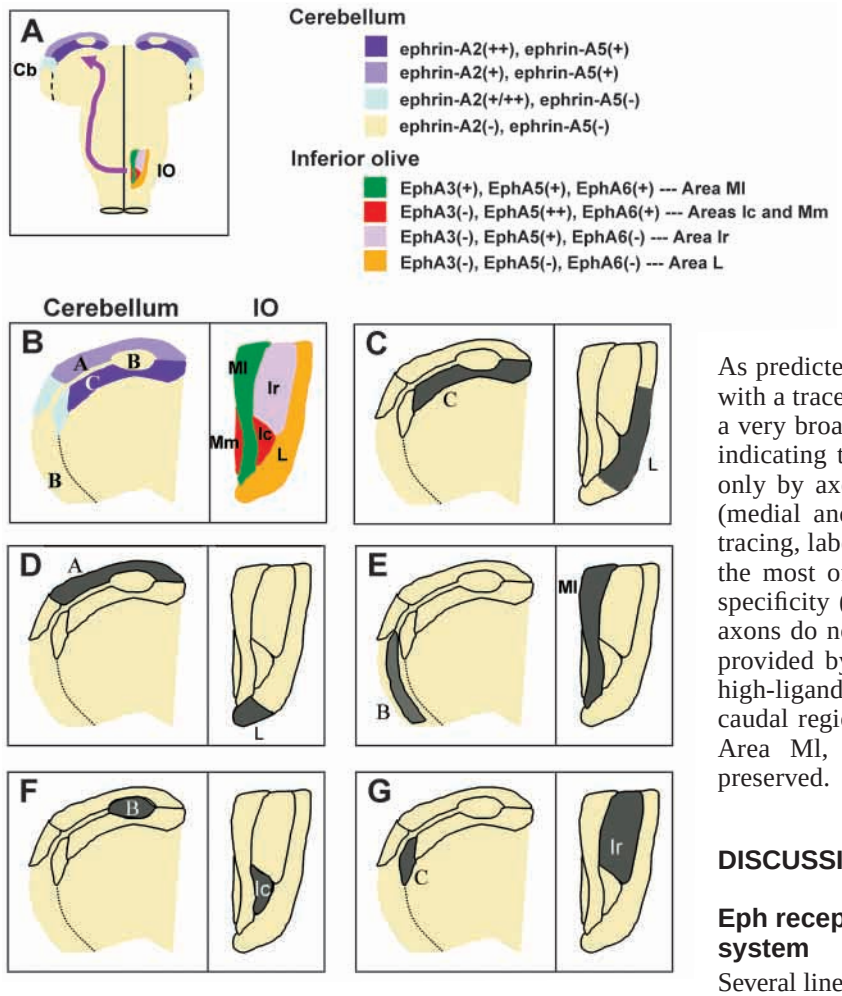

Fig. 7. Summary of the olivocerebellar topography and the Eph/ephrin domains. (A) Overview of the olivocerebellar projection in the organotypic hindbrain culture. (B) Cerebellar domains defined by ephrin-A ligands (left) and areas in the inferior olive defined by EphA receptors. (C-G) Corresponding areas between the cerebellum (left) and inferior olive (right) revealed in the axon tracing experiments are shown in grey.

receptors (EphA3, EphA4, EphA5, and EphA7) are expressed in distinct and overlapping domains of Purkinje cells (Karam et al., 2000; Lin and Cepko, 1998) (K. N. and M. N., unpublished). The expression patterns suggest that the receptor-ligand interaction could occur in developing cerebellum, raising the possibility that Eph receptors in the cerebellum could modulate the function of co-expressed ligands and thus affect the projection pattern. To test this, we used a retrovirus vector encoding the EphA3 receptor, which has high affinity both to ephrin-A2 and ephrin-A5. To reduce the risk that the misexpressed receptor itself transduces signals and exerts secondary effects, we used a truncated form of the EphA3 receptor in which most of the cytoplasmic domain is deleted (EphA3ΔC). Infection of the RCAS-EphA3ΔC virus caused a widespread expression of the receptor, which could be detected by affinity probe in situ with an ephrin-A2-AP probe (Fig. 8E). We then tested how the endogenous ephrin-A ligand activity was recognized after the retrovirus infection, using an EphA3-AP probe. Surprisingly, no ligand activity could be detected in cerebella infected with the EphA3ΔC virus (Fig. 8C), suggesting that the binding sites of endogenous ligands were occupied by the retrovirus-derived receptor.

If the binding sites of the endogenous ephrin-A ligands are occupied by the virus-derived EphA3ΔC receptor, one can expect that medial IO axons with high EphA receptors could now invade the high-ligand domains in the cerebellum. We tested this in axon tracing experiments using hindbrain explants infected with the RCAS-EphA3ΔC virus (Fig. 8M-O). As predicted, when the rostral part of domain C was marked with a tracer dye, retrogradely labeled cells were observed in a very broad area that covered most of the IO (22/25, 88%), indicating that this cerebellar domain was now invaded not only by axons from Area L, but also those from the other (medial and intermediate) areas of the IO. In anterograde tracing, labeled axons from Area Ml were found to project to the most of the cerebellum, without showing any domain-specificity (Fig. 8S,T). These results suggest that medial IO axons do not recognize the repulsive cues that are normally provided by ephrin-A ligands, and therefore can project to high-ligand domains in the cerebellum. Interestingly, the caudal region of domain B still receives axons mainly from Area Ml, indicating that some mapping order is still preserved.

DISCUSSION

Eph receptors and ephrins in the olivocerebellar system

Several lines of evidence in this study support the idea that the spatially accurate interaction between EphA receptors and ephrin-A ligands is essential for guiding IO axons to their target domains in the cerebellar cortex. First, EphA receptors and ephrin-A ligands are expressed with domain-specific patterns that correlate with olivocerebellar mapping domains. Receptor expression in the IO and ligand expression in the cerebellum have an inverse relationship; IO areas with no or low receptor activity project to cerebellar domains with high ligand activity, and vice versa. In addition, areas expressing different combinations of EphA receptors map to distinct cerebellar domains. Second, in vitro, ephrin-A2 inhibits axon outgrowth from the IO in an area-specific manner. Third, retroviral overexpression of *ephrin-A2* in the developing cerebellum results in disruption of the domain-specific mapping pattern, preventing axons with high EphA receptor expression from invading the ectopic expression domains. These results suggest that EphA receptors in IO axons and ephrin-A ligands in cerebellar target cells mediate repulsive/inhibitory signals, and act as domain-specific cues in target selection of the olivocerebellar projection.

Modulation of the ligand function and olivocerebellar map by co-expressed receptors

In the developing chicken cerebellum, not only ephrin-A ligands, but also EphA receptors are expressed in parasagittal domains of Purkinje cells. Since Purkinje cells send their axons to the deep cerebellar nuclei or the vestibular nuclei,

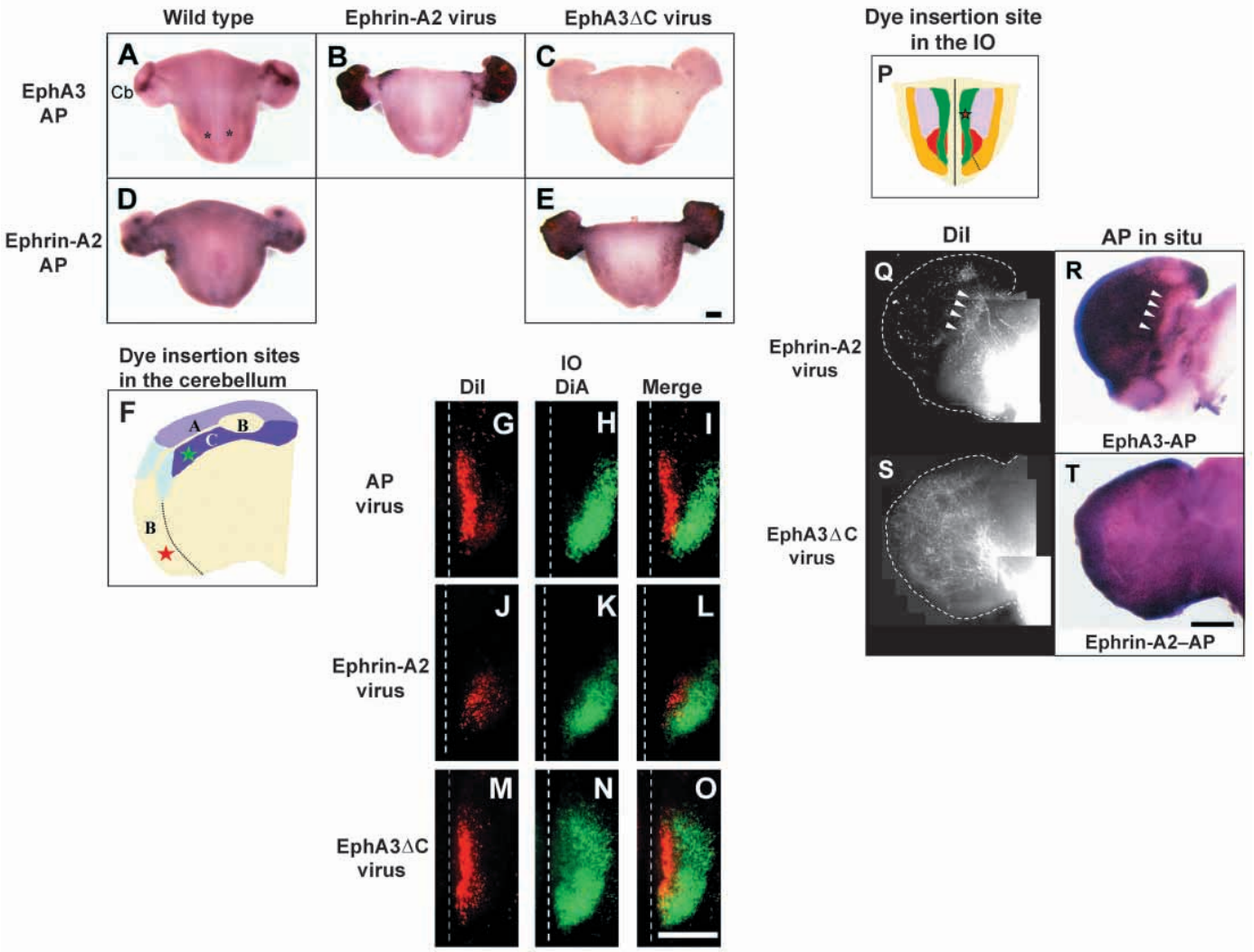

Fig. 8. Retroviral modification of the EphA-ephrin-A interaction in the cerebellum disrupts the olivocerebellar mapping. (A-E) Ligand and receptor activity detected by affinity probe in situ, in virus-infected explants. Rostral is at the top. Cb, cerebellum. Asterisk, inferior olive. (A) In an uninfected control cerebellum, parasagittal patterns of endogenous ligand activity are seen. (B) The cerebellum of an RCAS-ephrin-A2-infected embryo shows massive expression of *ephrin-A2*. (C) Following infection with the RCAS-EphA3ΔC virus, EphA3-AP fails to detect endogenous ligand activity. (D) Receptor activity in an uninfected control cerebellum. (E) Ectopic EphA3ΔC expression induced by the RCAS-EphA3ΔC virus. (F-O) Retrograde axon tracing in retrovirus-infected explants. (F) Dye insertion sites in the cerebellum of the organotypic hindbrain culture. The capital letters indicate domain names. The rostral domain C and the caudal domain B are labeled with DiA (green star) and DiI (red star), respectively. (G-I) Labeling pattern in the IO of an embryo infected with the RCAS-AP virus. The caudal domain B and the rostral domain C receive axons from Area Ml and Area L, respectively. (J-L) Representative labeling pattern of IO following infection with the RCAS-ephrin-A2 virus. The caudal domain B is invaded by axons from more lateral parts of the IO. The rostral domain C is innervated by axons from Area L. (M-O) In explants infected with the RCAS-EphA3ΔC virus, the caudal domain B receives axons from Area Ml. In contrast, the rostral domain C receives axons from broad areas of the IO. (P-T) Anterograde tracing of Area Ml axons in virus-infected explants. (P) DiI insertion site (Area Ml) in the IO. (Q-R) In explants infected with RCAS-ephrin-A2 virus, labeled axons stop at the border of ectopic expression domains (arrowheads), and fail to project to their normal target domain. (S-T) Following the RCAS-EphA3ΔC virus infection, Area Ml axons project to most parts of the cerebellum, including the domains with high endogenous ligand expression. Virus-derived expression was detected by affinity probe in situ (R,T). Scale bars, 500 μm.

one may expect that one of the major functions of EphA receptors in Purkinje cells is to act as axon guidance receptors to establish the olivonuclear and olivovestibular projections. While the present study does not directly address this issue, consistent with the prediction, region-specific expression of *ephrin-A2* and *ephrin-A5* were detected in the deep cerebellar nuclei by RNA in situ hybridization (K. N. and M. N., unpublished).

Results of the RCAS-EphA3ΔC retrovirus experiments suggest the possibility that EphA receptors in the cerebellum also play roles in the olivocerebellar mapping. First, the endogenous ligand activity in the cerebellum, which can normally be detected with EphA3-AP, becomes undetectable after overexpression of the EphA3ΔC receptor. Second, in those cerebella, medial IO axons with high receptor activity invade high ligand domains, which is consistent with the loss

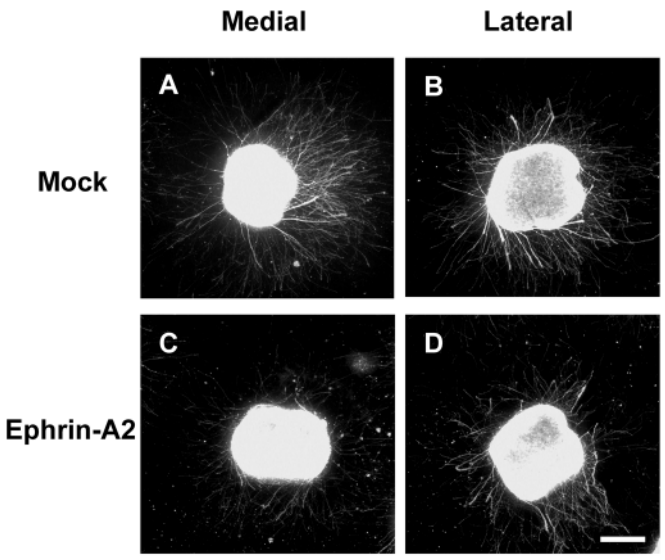

Fig. 9. Ephrin-A2 inhibits outgrowth of IO axons in vitro in a region-specific manner. Explants of the medial (A,C) and lateral (B,D) IO prepared from E8 embryos were grown on homogeneous carpets of 293T cell membrane, either mock-transfected (A,B), or transfected with pcDNA1-ephrin-A2 (C,D). Whereas axons from the lateral IO grow equally well on both membranes, axon outgrowth from the medial IO was significantly inhibited on the ephrin-A2 membrane. Scale bar, 500 μm.

of detectable ligand activity in the field. Although the present study did not directly test the function of endogenous Eph receptors, these findings suggest the possibility that endogenous receptors in the target field could function as a part of the positional information, by modulating the function of co-expressed ligands. In this regard, it is intriguing that in the middle part of domain C of the wild-type cerebellum, where several EphA receptors are co-expressed with *ephrin-A2*, the ligand activity detected with EphA3-AP was much weaker than expected from *ephrin-A2* RNA expression (Fig. 2D,E). Previous studies have shown that in the retinotectal system, the function of Eph receptors in the projecting field (retina) can be modulated by co-expressed ligands (Hornberger et al., 1999). Together with the present study, these findings suggest that in the Eph-ephrin system, the value of positional information in the projecting and target fields is determined through receptor-ligand interaction.

Whereas it has recently been shown that an ephrin-A ligand can transduce signals upon interaction with cognate EphA receptors (Davy et al., 1999), it is unlikely that overexpression of EphA3ΔC disrupted the projection pattern by mediating attractive or repulsive signals through ephrin-A ligands expressed on IO axons. First, in the wild-type embryo, expression and activity of ephrin-A ligands are localized in the lateral IO (K. N. and M. N., unpublished), which maps to cerebellar domains with low or no EphA receptor expression, and therefore does not fit the concept that the ligands on axons mediate attractive signals. Second, because axons from the lateral IO show massive innervation to the cerebella that overexpress EphA3ΔC, it is also unlikely that the ligands on axons mediate repulsive signals.

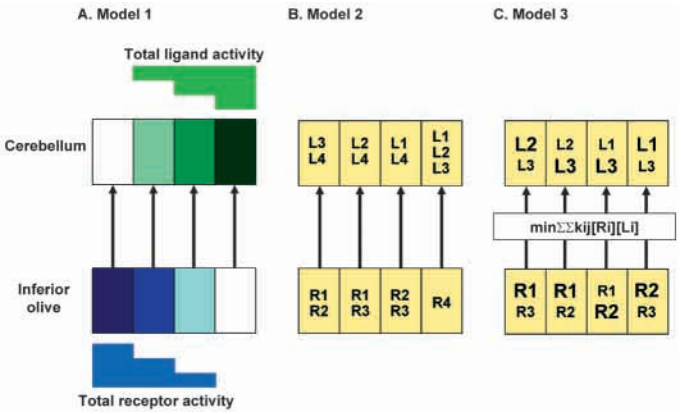

Fig. 10. Models for the mechanisms of the domain-specific olivocerebellar mapping. Schemes of the possible models discussed in the text are shown. R1-4, receptors; L1-4, ligands. Receptor-ligand pairs with the same numbers interact with high affinities. Large characters indicate high expression.

Mechanisms by which the Eph-ephrin system guides IO axons to the target domains

A variety of models could account for the mechanisms by which the Eph-ephrin system establishes the olivocerebellar target selection pattern. Some possible models are illustrated in Fig. 10. Because it is unlikely from our results that ephrin-A ligands act as axon attractants in this map, only models that involve repulsive or inhibitory signals are considered. In addition, when we discuss receptors and ligands in these models, they represent 'active' or 'unoccupied' portions.

In the first model (Fig. 10A), the mapping pattern is determined by the total amount of receptor activity on the growing axons and of ligand activity in the target domains, regardless of which or how many receptors contribute to the activity. Projecting areas with high receptor activity would be repelled from domains with high ligand activity, and would then map to no or low ligand domains. The activity crucial for target selection could either be absolute or relative amounts; the latter has been shown to be the case for Eph receptors in the retinocollicular projection (Brown et al., 2000). This model is compatible with our results that high areas of the receptor activity in the IO map to low domains of the ligand activity in the cerebellum, and vice versa.

In the second model (Fig. 10B), the projecting and target domains are characterized by combinations of receptors and ligands, respectively. This model is based on the assumption that in vivo, individual receptors could interact with a limited and distinct set of ligands. Then, axons would be arranged into distinct target domains through differential repulsion according to the receptor sets they express. In this regard, it is noteworthy that although the Eph-ephrin interaction shows promiscuity in in vitro binding assays, a recent study suggested that EphA receptors may interact with more selective set of ligands in vivo (Janis et al., 1999). This model seems to match some of our axon tracing results that cannot be clearly explained by the first model. For example, Areas Ml and Ic project to different cerebellar domains, although both areas contain comparable level of total receptor activity detected by ephrin-A2-AP. Different combinations of receptors are expressed in these

areas, and they may be responsible for the differential projections.

The third model is a combination of the concepts of the first and second models (Fig. 10C). In this model, the axons project to the target domain where they receive the minimal repulsive signal. The amount of repulsive signal may be determined by both expression levels of receptors/ligands and in vivo affinity of individual receptor-ligand pairs. As postulated in the mass action model (Nakamoto et al., 1996), the amount of repulsive signals could be most simply given as

$$\sum_i \sum_j \mathrm{Kij[Ri][Lj]} = \sum_i \sum_j \mathrm{[RiLj]}$$

(K, affinity constant; R, receptors on axons; L, ligands in a target domain; RL, receptor-ligand complex). Although further information on expression patterns of other Eph receptors and ephrins is necessary, at present we favor this model, because it is consistent with all the results obtained in this study.

The second and third models involve combinations of receptors and ligands acting as 'molecular codes' in target selection. This 'Eph code' model is also attractive in that it might explain why so many Eph receptors and ephrins exist in vertebrates. The large number of receptors and ligands, together with their complex expression patterns, might be required to make combinational molecular codes for the formation of the complex neuronal network. Intriguingly, it has been shown that combinations of the Robo receptor protein (the Robo code) expressed on axons are the major determinant of the position of longitudinal axon tracts in *Drosophila* (Rajagopalan et al., 2000; Simpson et al., 2000). Further studies, using gain- and loss-of-function approaches for each receptor and ligand, will be required to determine whether such 'Eph codes' exist and function, and which models can best explain the underlying mechanism for this complex neuronal projection.

Possible cooperation with other molecular mechanisms

Considering the complexity of the olivocerebellar map, it seems likely that in addition to the Eph-ephrin system, other molecular systems are also involved in the selection of target domains. For example, the models in Fig. 10 do not explain how the incoming axons detect the correct direction to grow within the cerebellum. In addition, model 1 has the problem of explaining why axons with no receptors map to the high-ligand target domains. These issues could be explained, for example, by considering other classes of molecules, such as domain-specific attractants or adhesion molecules that interact with specific subsets of IO axons, and other domain-specific repellent system. Interestingly, in the cerebellum infected with the RCAS-EphA3ΔC virus, the caudal domain B is still innervated by Area Ml axons (Fig. 8M,O), which might be suggesting involvement of other molecular systems. A number of molecules, including semaphorins (Rabacchi et al., 1999), cadherins (Arndt et al., 1998; Hirano et al., 1999), and an immunoglobulin family member BEN/SC-1 (Chédotal et al., 1996), have been shown to be expressed in specific mapping domains of the olivocerebellar system. While it is not clear yet whether these molecules could be involved in the olivocerebellar mapping, their domain-specific expression does suggest possible functions in patterning this complex projection.

We thank Karl Herrup, Hiroshi Matsuoka, and Hiroya Obama for help and advice, and Wendy Macklin and Mark Perin for discussions and comments on the manuscript. This work was supported by National Institutes of Health grants (J. G. F., M.N.), a Fellowship from the Klingenstein foundation (J. G. F.), and grants from March of Dimes Birth Defects Foundation and Whitehall Foundation (M. N.).

REFERENCES

Altman, J. and Bayer, S. A. (1997). Development of the Cerebellar System: In Relation to its Evolution, Structure, and Functions. New York: CRC Press.

Arndt, K., Nakagawa, S., Takeichi, M. and Redies, C. (1998). Cadherin-defined segments and parasagittal cell ribbons in the developing chicken cerebellum. *Mol. Cell Neurosci.* **10**, 211-228.

Brodal, A. and Kawamura, K. (1980). Olivocerebellar projection: A review. *Adv. Anat. Embryol. Cell Biol.* **64**, 1-140.

Brown, A., Yates, P. A., Burrola, P., Ortuno, D., Vaidya, A., Jessell, T. M., Pfaff, S. L., O'Leary, D. D. and Lemke, G. (2000). Topographic mapping from the retina to the midbrain is controlled by relative but not absolute levels of EphA receptor signaling. *Cell* **102**, 77-88.

Buisseret-Delmas, C. and Angaut, P. (1993). The cerebellar olivo-corticonuclear connections in the rat. *Prog. Neurobiol.* **40**, 63-87.

Chédotal, A., Bloch-Gallego, E. and Sotelo, C. (1997). The embryonic cerebellum contains topographic cues that guide developing inferior olivary axons. *Development* **124**, 861-870.

Chédotal, A., Pourquie, O., Ezan, F., San Clemente, H. and Sotelo, C. (1996). BEN as a presumptive target recognition molecule during the development of the olivocerebellar system. *J. Neurosci.* **16**, 3296-3310.

Cheng, H. J., Nakamoto, M., Bergemann, A. D. and Flanagan, J. G. (1995). Complementary gradients in expression and binding of ELF-1 and Mek4 in development of the topographic retinotectal projection map. *Cell* **82**, 371-381.

Crowley, J. C. and Katz, L. C. (2000). Early development of ocular dominance columns. *Science* **290**, 1321-1324.

Davy, A., Gale, N. W., Murray, E. W., Klinghoffer, R. A., Soriano, P., Feuerstein, C. and Robbins, S. M. (1999). Compartmentalized signaling by GPI-anchored ephrin-A5 requires the Fyn tyrosine kinase to regulate cellular adhesion. *Genes Dev.* **13**, 3125-3135.

Drescher, U., Kremoser, C., Handwerker, C., Loschinger, J., Noda, M. and Bonhoeffer, F. (1995). In vitro guidance of retinal ganglion cell axons by RAGS, a 25 kDa tectal protein related to ligands for Eph receptor tyrosine kinases. *Cell* **82**, 359-370.

Eph Nomenclature Committee (1997). Unified nomenclature for Eph family receptors and their ligands, the ephrins. *Cell* **90**, 403-404.

Fekete, D. M. and Cepko, C. L. (1993a). Replication-competent retroviral vectors encoding alkaline phosphatase reveal spatial restriction of viral gene expression/transduction in the chick embryo. *Mol. Cell. Biol.* **13**, 2604-2613.

Fekete, D. M. and Cepko, C. L. (1993b). Retroviral infection coupled with tissue transplantation limits gene transfer in the chicken embryo. *Proc. Natl. Acad. Sci. USA* **90**, 2350-2354.

Feldheim, D. A., Kim, Y. I., Bergemann, A. D., Frisén, J., Barbacid, M. and Flanagan, J. G. (2000). Genetic analysis of ephrin-A2 and ephrin-A5 shows their requirement in multiple aspects of retinocollicular mapping. *Neuron* **25**, 563-574.

Flanagan, J. G. and Vanderhaeghen, P. (1998). The ephrins and Eph receptors in neural development. *Annu. Rev. Neurosci.* **21**, 309-345.

Frisén, J., Yates, P. A., McLaughlin, T., Friedman, G. C., O'Leary, D. D. and Barbacid, M. (1998). Ephrin-A5 (AL-1/RAGS) is essential for proper retinal axon guidance and topographic mapping in the mammalian visual system. *Neuron* **20**, 235-243.

Furber, S. E. (1983). The organization of the olivocerebellar projection in the chicken. *Brain Behav. Evol.* **22**, 198-211.

Furber, S. E. and Watson, C. R. (1983). Organization of the olivocerebellar projection in the rat. *Brain Behav. Evol.* **22**, 132-152.

Hirano, S., Yan, Q. and Suzuki, S. T. (1999). Expression of a novel

protocadherin, OL-protocadherin, in a subset of functional systems of the developing mouse brain. *J. Neurosci.* **19**, 995-1005.

Hornberger, M. R., Dutting, D., Ciossek, T., Yamada, T., Handwerker, C., Lang, S., Weth, F., Huf, J., Wessel, R., Logan, C. et al. (1999). Modulation of EphA receptor function by coexpressed ephrinA ligands on retinal ganglion cell axons. *Neuron* **22**, 731-742.

Janis, L. S., Cassidy, R. M. and Kromer, L. F. (1999). Ephrin-A binding and EphA receptor expression delineate the matrix compartment of the striatum. *J. Neurosci.* **19**, 4962-4971.

Karam, S. D., Burrows, R. C., Logan, C., Koblar, S., Pasquale, E. B. and Bothwell, M. (2000). Eph receptors and ephrins in the developing chick cerebellum: relationship to sagittal patterning and granule cell migration. *J. Neurosci.* **20**, 6488-6500.

Lin, J. C. and Cepko, C. L. (1998). Granule cell raphes and parasagittal domains of Purkinje cells: complementary patterns in the developing chick cerebellum. *J. Neurosci.* **18**, 9342-9353.

Menzel, P., Valencia, F., Godement, P., Dodelet, V. C. and Pasquale, E. B. (2001). Ephrin-A6, a new ligand for EphA receptors in the developing visual system. *Dev. Biol.* **230**, 74-88.

Monschau, B., Kremoser, C., Ohta, K., Tanaka, H., Kaneko, T., Yamada, T., Handwerker, C., Hornberger, M. R., Loschinger, J., Pasquale, E. B. et al. (1997). Shared and distinct functions of RAGS and ELF-1 in guiding retinal axons. *EMBO J.* **16**, 1258-1267.

Nakamoto, M., Cheng, H. J., Friedman, G. C., McLaughlin, T., Hansen, M. J., Yoon, C. H., O'Leary, D. D. and Flanagan, J. G. (1996). Topographically specific effects of ELF-1 on retinal axon guidance in vitro and retinal axon mapping in vivo. *Cell* **86**, 755-766.

Rabacchi, S. A., Solowska, J. M., Kruk, B., Luo, Y., Raper, J. A. and Baird, D. H. (1999). Collapsin-1/semaphorin-III/D is regulated developmentally in Purkinje cells and collapses pontocerebellar mossy fiber neuronal growth cones. *J. Neurosci.* **19**, 4437-4448.

Rajagopalan, S., Vivancos, V., Nicolas, E. and Dickson, B. J. (2000). Selecting a longitudinal pathway: Robo receptors specify the lateral position of axons in the Drosophila CNS. *Cell* **103**, 1033-1045.

Sajjadi, F. G., Pasquale, E. B. and Subramani, S. (1991). Identification of a new eph-related receptor tyrosine kinase gene from mouse and chicken that is developmentally regulated and encodes at least two forms of the receptor. *New Biol.* **3**, 769-778.

Siever, D. A. and Verderame, M. F. (1994). Identification of a complete Cek7 receptor protein tyrosine kinase coding sequence and cDNAs of alternatively spliced transcripts. *Gene* **148**, 219-226.

Simpson, J. H., Bland, K. S., Fetter, R. D. and Goodman, C. S. (2000). Short-range and long-range guidance by Slit and its Robo receptors: a combinatorial code of Robo receptors controls lateral position. *Cell* **103**, 1019-1032.

Sotelo, C. and Chédotal, A. (1997). Development of the olivocerebellar projection. *Perspect. Dev. Neurobiol.* **5**, 57-67.

Sperry, R. W. (1963). Chemoaffinity in the orderly growth of nerve fiber patterns and connections. *Proc. Natl. Acad. Sci. USA* **50**, 703-710.

Thanos, S. and Mey, J. (2001). Development of the visual system of the chick. II. Mechanisms of axonal guidance. *Brain Res. Brain Res. Rev.* **35**, 205-245.

Walter, J., Kern-Veits, B., Huf, J., Stolze, B. and Bonhoeffer, F. (1987). Recognition of position-specific properties of tectal cell membranes by retinal axons in vitro. *Development* **101**, 685-696.

Wassef, M., Cholley, B., Heizmann, C. W. and Sotelo, C. (1992). Development of the olivocerebellar projection in the rat: II. Matching of the developmental compartmentations of the cerebellum and inferior olive through the projection map. *J. Comp. Neurol.* **323**, 537-550.